Journal of Non-Crystalline Solids 540 (2020) 120011

Contents lists available at ScienceDirect

Journal of Non-Crystalline Solids

journal homepage: www.elsevier.com/locate/jnoncrysol

Vibrational study of lithium borotellurite glasses

K.I. Chatzipanagis[a], N.S. Tagiara[a], D. Möncke[b], S. Kundu[c], A.C.M. Rodrigues[c], E.I. Kamitsos[a,*]

[a] Theoretical and Physical Chemistry Institute, National Hellenic Research Foundation, 48 Vassileos Constantinou Ave., Athens 116 35, Greece
[b] Inamori School of Engineering at the New York State College of Ceramics, Alfred University, 1 Saxon Drive, Alfred, New York 14802, United States
[c] Federal University of São Carlos, Department of Materials Engineering, CP 676, São Carlos, SP 13565-905, Brazil

ARTICLE INFO

Keywords:
Lithium borotellurite glasses
Raman spectroscopy
IR reflectance spectroscopy

ABSTRACT

Ion-conducting lithium borotellurite glasses of composition $(Li_2O)_y$-$[(2TeO_2)_x$-$(B_2O_3)_{1-x}]_{1-y}$ ($y = 0.33$ and 0.40 and $0 \leq x \leq 1$) were investigated by Raman and infrared (IR) techniques. The Raman spectra demonstrated the transition from TeO_4 trigonal bipyramid (tbp's) units to TeO_3 trigonal pyramids (tp's) with terminal oxygens upon increasing B_2O_3 content, but gave minimal information for the borate species due to their weak scattering efficiency relative to the tellurite species. In contrast, IR spectroscopy was very effective in probing the vibrational response of borate tetrahedra and triangles. Upon increase of tellurite content, the borate tetrahedra showed enhanced absorption relative to borate triangles, this result being in line with an increased fraction of borate tetrahedra seen in previous NMR studies. Raman and IR results are interpreted in the context of weak Te…O-B interactions, through which tellurium oxide acts as a second modifier next to Li_2O and leads to an enhanced formation of borate tetrahedral units.

1. Introduction

Tellurite glasses are known to display interesting properties such as high refractive index, good infrared transmittance, high dielectric constant and low temperature of melting and, thus, their use can span across a broad range of technological applications comprising optical recording media, optical switching devices, Raman amplification etc. [1–4]. Concurrently, lithium borate based glasses have been extensively investigated over the years due to their high ionic conductivity, which ultimately makes them prominent candidates for the design of efficient solid electrolytes in energy storage applications [5–9]. Hence, it is feasible to achieve fine-tuning of physical, optical and electrical properties by mixing the tellurite and borate network forming oxides. Such mixing leads to non-linear variations in the ionic conductivity and glass transition temperature with composition, a phenomenon known as the mixed network former effect [10,11].

The implications of such network former mixing are enhanced by the presence of the glass modifier ions [12]. As a result, important questions arise concerning the degree of sharing of the modifier ions among the two network formers and the extent of the interactions between the two glass sub-networks. Such questions have been recently addressed for Na-tellurite-phosphate glasses $(Na_2O)_{1/3}$-$[(2TeO_2)_x$-$(P_2O_5)_{1-x}]_{2/3}$ [13], Na-tellurite-borates $(Na_2O)_{1/3}$-$[(2TeO_2)_x$-$(B_2O_3)_{1-x}]_{2/3}$ [14] and Li-tellurite-borate glasses $(Li_2O)_y$-$[(2TeO_2)_x$-$(B_2O_3)_{1-x}]_{1-y}$ [15]. The tellurite-phosphate system was found to exhibit a positive mixed network former effect in both glass transition temperature and ionic conductivity [13], in contrast to the two tellurite-borate glass systems which show a negative mixed network former effect [14,15]. Possible structural origins of these opposite behaviours were investigated by spectroscopic techniques including solid-state nuclear magnetic resonance (NMR) and X-ray photoelectron spectroscopy (XPS). Thus, it was concluded that the positive mixed network former effect is associated with the preferential formation of heteroatomic linkages, e.g. Te-O-P [13], while the data for tellurite-borate glasses were interpreted in terms of a tendency for avoidance of Te-O-B bridges, indicating some degree of chemical segregation into binary Na (Li)-borate and Na(Li)-tellurite domains [14,15].

Besides NMR, Raman and infrared (IR) vibrational spectroscopic techniques can provide insights into the structural mechanisms controlling the properties of ternary glasses. Binary lithium-tellurite and lithium-borate glasses have been already studied by means of vibrational spectroscopy. In particular, Raman spectra of lithium-tellurite and other metal oxide containing tellurite glasses have clearly demonstrated that upon increasing the metal oxide content there is a gradual conversion of TeO_4 trigonal bi-pyramids (tbp's) into TeO_{3+1} polyhedra with one or two terminal oxygen atoms, which further transform into TeO_3^{2-} trigonal pyramids (tp's) with all oxygen atoms being terminal at relatively high amounts of metal oxide [16–20]. In parallel, Raman studies on lithium-

* Corresponding author.
E-mail address: eikam@eie.gr (E.I. Kamitsos).

https://doi.org/10.1016/j.jnoncrysol.2020.120011
Received 12 November 2019; Received in revised form 26 February 2020; Accepted 29 February 2020
Available online 04 May 2020
0022-3093/ © 2020 Elsevier B.V. All rights reserved.

and other alkali-borate glasses have shown that the boroxol rings in vitreous B_2O_3 are gradually modified through conversion of neutral trigonal $BO_{3/2}$ ($O_{1/2}$ denotes bridging oxygen) units into tetrahedral $[BO_{4/2}]^-$ units due to the addition of alkali oxide, leading initially to the development of large superstructural units (e.g. pentaborates) and, subsequently, to anionic triangular borate units with increasing number of terminal oxygen atoms [12,21,22]. These and related studies [23–26] have shown that, Raman spectroscopy is a powerful method for probing boroxol rings as well as the formation of non-bridging oxygens (NBO's) in modified borate glasses.

The knowledge on the structural evolution observed by Raman spectroscopy is complemented by IR studies on the same glasses. For Li-borate glasses in particular, the IR spectra display distinct absorption bands assigned to borate triangular and tetrahedral species, and these spectral features facilitate the quantification of boron speciation [7,24–26] even for borate glasses containing paramagnetic ions like Mn^{2+} and Cu^{2+} for which no NMR data are available [26]. Compared to the rich infrared data available for Li-borate glasses, no infrared spectra have been reported for Li-tellurite glasses to the best of our knowledge.

Considering the existing knowledge on binary Li-borate and tellurite glasses and the effectiveness of both vibrational spectroscopies, we employed here these techniques on ternary lithium boro-tellurite glasses to enhance our understanding on the structural interplay between the borate and tellurite sub-networks, in light of the NMR work performed by Oliveira et al. on the same glass samples [15].

2. Materials and experimental methods

2.1. Glass samples

Two series of lithium borotellurite glasses of composition $(Li_2O)_y$-$[(2TeO_2)_x$-$(B_2O_3)_{1-x}]_{1-y}$ with $y = 0.33$ and 0.40 were synthesized using the conventional melt quenching technique [15]. Appropriate quantities of the reactants (Li_2CO_3, H_3BO_3 and TeO_2) were mixed in powder form and heated in a platinum crucible at temperature varying from 700 to 1000 °C depending on composition. The melt was subsequently splat-quenched on a stainless-steel plate at room temperature and the formed glasses were then annealed at a temperature of Tg − 50 °C for 4 h. Further details regarding the synthesis of these glasses can be found in the work of Oliveira et al. [15]. Prior to spectroscopic measurement, samples were polished to produce smooth surfaces suitable for high quality IR reflectance spectra.

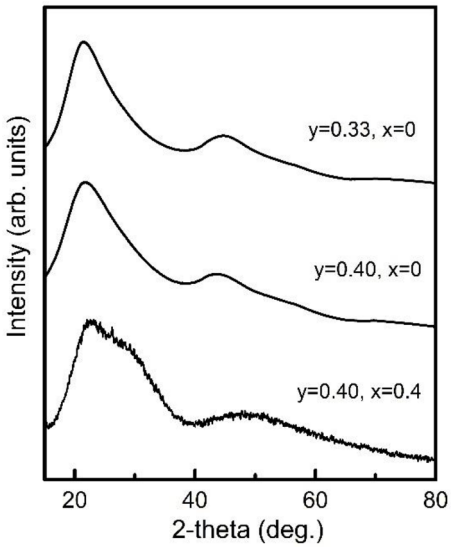

Fig. 1. XRD patterns of representative glass compositions $(Li_2O)_y$-$[(2TeO_2)_x$-$(B_2O_3)_{1-x}]_{1-y}$ with $y = 0.33$, $x = 0$; $y = 0.40$, $x = 0$; $y = 0.40$, $x = 0.4$.

2.2. X-ray diffraction

The amorphous nature of lithium borotellurite samples was confirmed by X-ray diffraction (XRD) measurements. They were carried out on powders of representative glass compositions with Cu Kα radiation, angular range $15.0 \le 2\theta/^\circ \le 80.0$ and 120 s exposure (Agilent Technologies, $\lambda = 1.5418$ Å, with X-rays being generated at 50 kV and 0.8 mA). The XRD patterns shown in Fig. 1 are characterized by broad halos which are typical of fully amorphous materials, in agreement with reported XRD patterns of lithium-borate [27] and borotellurite [28] glasses. In addition, the broad XRD patterns are in line with the Raman spectra of this work (Fig. 2), which are also free of sharp peaks characterizing crystalline compounds.

2.3. Spectroscopic techniques

Raman spectra were measured under backscattering geometry on a Renishaw inVia Raman Microscope, using the 514.5 nm line of an Ar ion laser for excitation. All spectra were recorded at room temperature with 4 cm^{-1} spectral resolution. A 50x long working distance lens was employed to form a laser spot diameter of 2–3 μm on the sample, with no signs of laser-induced modifications being observed.

Infrared spectra were measured on a vacuum Fourier transform spectrometer (Bruker, Vertex 80v), in quasi-specular reflectance mode (11° off-normal). Reflectance spectra were separately recorded in the far-IR (2000 scans averaged) and mid-IR range (400 scans averaged) and then merged to form a continuous spectrum in the range 30–7000 cm^{-1}. All spectra were measured against a high reflectivity gold mirror at room temperature with 4 cm^{-1} resolution. Analysis of reflectance spectra by Kramers–Kronig transformation yielded the absorption coefficient spectra, $a(\nu)$, from the expression $a(\nu) = 4\pi\nu k(\nu)$ where ν is the infrared frequency in cm^{-1} and $k(\nu)$ is the imaginary part of the complex refractive index [29].

3. Results

The unpolarized Raman spectra of lithium borotellurite glasses $(Li_2O)_y$-$[(2TeO_2)_x$-$(B_2O_3)_{1-x}]_{1-y}$ for $y = 0.33$ and 0.40 are shown in Fig. 2a and b, respectively, as a function of tellurite content (x). The Raman spectra of pure Li-tellurite glasses in Fig. 2a ($x = 1$, $0.2Li_2O$-$0.8TeO_2$) and Fig. 2b ($x = 1$, $0.25Li_2O$-$0.75TeO_2$) are in very good agreement with those reported for glasses having the same [16] or similar compositions [17,18]. For both glass series, the addition of B_2O_3 leads to the gradual destruction of the tellurite network as manifested by the decrease in intensity of the tellurite bands at about 460 and 665 cm^{-1}, while the concomitant development of the bands at about 770 cm^{-1} mark the gradual formation of the borate network.

The Raman spectra of binary Li-borate glasses in Fig. 2a ($x = 0$, $0.33Li_2O$-$0.67B_2O_3$) and Fig. 2b ($x = 0$, $0.40Li_2O$-$0.60B_2O_3$) exhibit their most prominent band at ~770 cm^{-1} and are in very good agreement with reported spectra [21,22]. Besides the strong and sharp bands at ~770 cm^{-1}, the Li-borate glasses exhibit weaker and broader features at 505–528 cm^{-1}, ~660 cm^{-1}, 955–1000 cm^{-1}, 1125 cm^{-1} and 1430–1470 cm^{-1}. These weaker borate bands are strongly reduced in intensity in the spectra of the ternary glasses, even in those at $x = 0.2$ glass compositions which contain 80% B_2O_3. This apparent disproportional reduction in the Raman activity of borate-related bands in Fig. 2 should originate from the large difference in polarizability, α, between the Te^{4+} and B^{3+} ions, $\alpha_{Te^{4+}} = 1.595$ Å^3 and $\alpha_{B^{3+}} = 0.002$ Å^3 [30], which makes the Te-O bond much more polarizable than the B-O bond and, thus, leads to large differences in the Raman cross section between tellurite and borate vibrational modes. This should hold with the exception of the breathing mode of borate rings with $[BO_{4/2}]^-$ tetrahedra at ~770 cm^{-1}, involving mainly the three oxygen atoms within the ring [21,22]. Because of its totally symmetric and completely localized character, this mode has a high Raman cross section and gives rise to

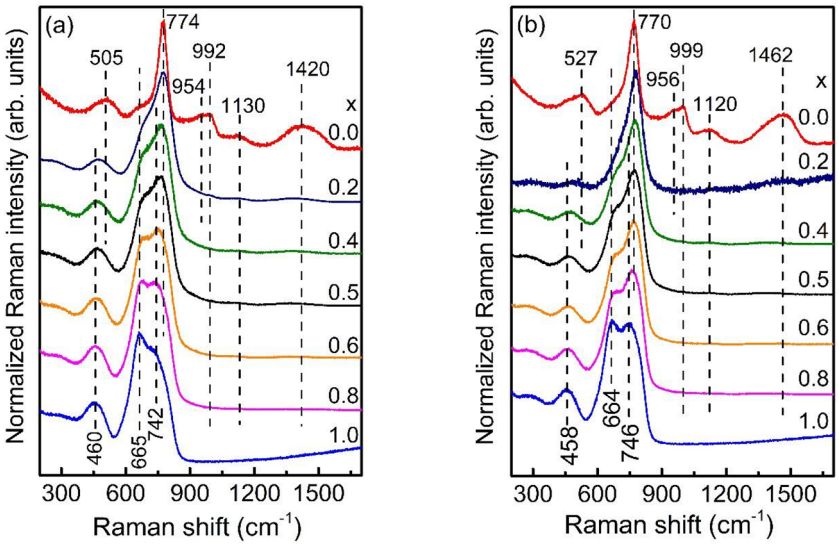

Fig. 2. Unpolarized Raman spectra of glasses $(Li_2O)_y$-$[(2TeO_2)_x$-$(B_2O_3)_{1-x}]_{1-y}$ for $y = 0.33$ (a) and $y = 0.40$ (b).

relatively sharp bands like the breathing mode of boroxol rings at 805 cm^{-1} [31,32]. Due to such limitations, it is difficult to extract from the Raman spectra alone information on the possible changes of boron speciation in the presence of tellurite species.

An alternative method to probe the boron speciation is IR spectroscopy, where changes in the dipole moment of the vibrating structural units determine their activity. The IR spectra of Li-borotellurite glasses with $y = 0.33$ and 0.40 are depicted in Fig. 3a and b, respectively. The IR spectra of the binary Li-tellurite glasses ($x = 1$) show a broad absorption band in the far-IR region (below ~530 cm^{-1}) and a strong absorption envelope in the mid-IR, with its strongest component at 625–635 cm^{-1} and shoulders at ~690–700 cm^{-1} and ~760 cm^{-1}.

direct evidence for the presence of borate species.

The envelops at ~940 and 1330 cm^{-1} gain relative intensity upon increasing the B_2O_3 content, and become the main absorption profiles of the end-member Li-borate glasses in Fig. 3a ($x = 0$: $0.33Li_2O$-$0.67B_2O_3$) and Fig. 3b ($x = 0$: $0.40Li_2O$-$0.60B_2O_3$). The spectra of these binary Li-borate glasses are in good agreement with reported data for the same glass compositions [7].

As observed in Fig. 3a and b, the mixing of the two glass former oxides in the ternary compositions affects both the borate and tellurite characteristic bands. The most profound changes include the upshift in frequency of the ~940 and 1330 cm^{-1} borate features to about 995–1042 and 1377–1380 cm^{-1}, and the intensity increase of the

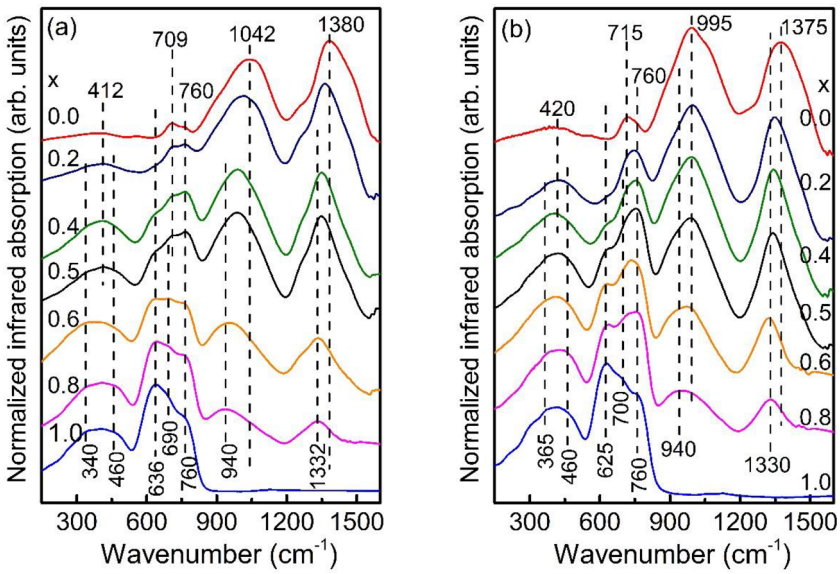

Fig. 3. IR spectra of $(Li_2O)_y$-$[(2TeO_2)_x$-$(B_2O_3)_{1-x}]_{1-y}$ glasses for $y = 0.33$ (a) and $y = 0.40$ (b).

Addition of B_2O_3 causes the appearance of two new absorption envelopes peaking initially at about 940 and 1330 cm^{-1}, where there is no infrared activity of tellurite species. Clearly, these new IR features signal the presence of borate units already at 20 mol% B_2O_3 ($x = 0.8$). In comparison, the corresponding Raman spectra at $x = 0.8$ are dominated by the much intense scattering of the tellurite units and give no tellurite shoulders at ~690–700 cm^{-1} and ~760 cm^{-1} over the 625–635 cm^{-1} band as the B_2O_3 content increases (decreasing x). These spectral variations show clearly that the tellurite and borate subnetworks are both influenced by mixing and this aspect will be discussed in the next section.

4. Discussion

4.1. Raman spectroscopy

The Raman spectra of Li-tellurite glasses in Fig. 2a and b ($x = 1$) exhibit a strong feature at 665 cm^{-1} attributed to stretching vibrations of TeO_4 tbp's, a shoulder at ~745 cm^{-1} corresponding to the stretching of TeO_{3+1} polyhedra with terminal oxygen atoms, and a weak component at 460 cm^{-1} assigned to stretching-bending vibration of Te-O-Te bridges [17–20,33,34]. A noticeable difference among the spectra of the two Li-tellurite glasses is the relative intensity of the 745 cm^{-1} feature which appears more pronounced in the $0.25Li_2O$-$0.75TeO_2$ glass (Fig. 2b), suggesting an increased fraction of TeO_{3+1} units as a result of the higher Li_2O concentration. Addition of B_2O_3 causes the progressive reduction in intensity of the 665 cm^{-1} band. This is followed initially by the strengthening of the 745 cm^{-1} shoulder, and then the growing of a new band at ~770 cm^{-1}; the latter feature indicates the formation of TeO_3 units with terminal oxygen atoms [17,34]. Therefore, increasing the B_2O_3/TeO_2 ratio in these ternary glasses appears to trigger the transformation $TeO_4 \rightarrow TeO_{3+1} \rightarrow TeO_3$, despite the fact that the Li_2O content is kept constant. For $x = 0$, the Raman spectra of the Li-borate glasses display their strongest band at ~770 cm^{-1} (Fig. 2a,b). The breathing vibration of borate rings containing two trigonal $BO_{3/2}$ units and one tetrahedral $[BO_{4/2}]^-$ unit was measured at 780 cm^{-1}, while the corresponding mode of borate rings with one $BO_{3/2}$ and two $[BO_{4/2}]^-$ units was found to scatter at 760 cm^{-1} in Li-borate glasses [23]. Therefore, the ~770 cm^{-1} in Fig. 2a and b indicates the coexistence of borate rings with one and two $[BO_{4/2}]^-$ units, and corresponding numbers of $BO_{3/2}$ units [22,23]. Weaker features located in the region of 950–1000 cm^{-1} are generally attributed to the asymmetric stretching vibration of borate tetrahedra in superstructural groups like pentaborate and tetraborate, while the very weak band at about 1120 cm^{-1} can be associated to diborate groups [22]. The low frequency band at about 505–530 cm^{-1} designates also the presence of $[BO_{4/2}]^-$ units in superstructural groups (pentaborate, tetraborate and diborate). The broad-band structure centered at ~1420 cm^{-1} (Fig. 2a) or ~1460 cm^{-1} (Fig. 2b) is attributed to boron-oxygen stretching vibrations, including B-O^- stretching in metaborate triangles $BO_{2/2}O^-$ attached to large borate groups [22,23]. Finally, the lack of sufficient Raman signal at ~930, 840 and 1250 cm^{-1} denotes the absence of detectable concentration of orthoborate and pyroborate units [22]. As observed in Fig. 2, minor additions of the tellurite component led to the severe diminishing of the weak borate bands because of the strong polarizability of the tellurite vibration modes. Also, there is substantial overlapping of the stretching frequency of TeO_3 units containing terminal oxygens with the strong breathing mode of the six-membered borate rings, making difficult the separation of their contributions to the total Raman signal measured at ~770 cm^{-1}.

Raman and IR study by Rong et al. on the binary glass system zB_2O_3-(1-z)TeO_2 ($0 < z \leq 0.275$) reported the absence of TeO_3 units with terminal oxygen atoms and the formation of discrete $BO_{3/2}$ and $[BO_{4/2}]^-$ units, i.e. the absence of large borate structures [16]. A Raman study by Sekiya et al. [33] on the same binary glasses suggested the formation of TeO_3 tps, as well as of discrete $[BO_{4/2}]^-$ units and small amounts of pyroborate and orthoborate units. The conversion of TeO_4 tbp's to TeO_3 tp's was also suggested by Raman spectroscopy on ternary sodium-borotellurite glasses where the sodium content was held constant [14].

In summarizing this section we note that our Raman results on $(Li_2O)_y$-$[(2TeO_2)_x$-$(B_2O_3)_{1-x}]_{1-y}$ glass show the progressive transformation of TeO_4 tbp's to TeO_{3+1} units and to TeO_3 tp's with terminal oxygen atoms upon increasing B_2O_3 content, although the lithium oxide content is held constant in each series. This interesting result may indicate some kind of interaction among the two glass formers and this will be discussed later. Also, the strong Raman scattering of the tellurite units renders the structural investigation of the borate network cumbersome and, thus, IR spectroscopy was employed to overcome this hindrance.

4.2. IR spectroscopy

The IR spectra of Li-tellurite glasses in Fig. 3a and b ($x = 1$) exhibit a strong band at ~630 cm^{-1} attributed to the stretching vibrations of TeO_4 tbp's, weaker features at ~690 and 760 cm^{-1} denoting the stretching of TeO_{3+1} and TeO_3 structural units, and weaker contributions at about 460 cm^{-1} assigned to the bending of Te-O-Te bridges [34]. Low-frequency shoulders at about 340 cm^{-1} (Fig. 3a) and 365 cm^{-1} (Fig. 3b) may arise from the vibration of Li cations against their anionic tellurite sites, ν(Li-O), in analogy to Li-O vibrations measured in other oxide glasses [35]. The addition of B_2O_3 causes an intensity reduction of the 630 cm^{-1} band indicating the progressive destruction of TeO_4 units, whereas the bands at ~690 and 760 cm^{-1} gain intensity, thus signaling the formation of TeO_{3+1} and TeO_3 units with terminal oxygen atoms. Therefore, the composition dependence of the IR bands assigned to tellurite units is in very good agreement with the evolution of the corresponding Raman spectra; both confirming the reduction in the coordination number of tellurium from 4 to 3 upon addition of B_2O_3.

The Li-borate glasses ($x = 0$) exhibit IR absorption predominantly in three regions: 650–800 cm^{-1} ascribed to the bending motions of borate units, 800–1200 cm^{-1} assigned to B-O stretching vibrations of borate tetrahedra and 1200–1550 cm^{-1} attributed to B-O stretching vibrations of borate trigonal units [7]. As observed in Fig. 3, the band envelop related to borate tetrahedra downshifts from about 1042 to 995 cm^{-1} upon increasing modification of the borate network from $0.33Li_2O$-$0.67B_2O_3$ to $0.40Li_2O$-$0.60B_2O_3$. Similarly, the absorption envelop of borate triangular units downshifts from about 1380 to 1375 cm^{-1} upon increasing Li_2O content (i.e. from $y = 0.33$ to $y = 0.40$). These spectral changes manifest variations in the environment of borate tetrahedral and triangular units as modification increases in the binary Li-borate glasses. The incorporation of TeO_2 in the two borate glass systems at constant Li_2O content ($y = 0.33$, 0.40) leads to further spectral alterations of the borate absorption envelopes, including changes in their shape and large frequency shifts. The borate tetrahedral and triangular absorption envelops appear now at about 940 and 1330 cm^{-1} for $x = 0.8$. Considering the absence of tellurite absorption above 900 cm^{-1}, the borate tetrahedral units appear to prevail at increasing TeO_2 content (Fig. 3a and b). Taken together, these results manifest the gradual change in the nature and relative population of the borate species with addition of TeO_2. It has been previously suggested that the presence of the large tellurium atoms facilitates the breaking down of the rigid Li-borate network [36], whereas a subsequent increase in the molar volume of the present glasses was observed at increasing TeO_2 [15]. The superstructural units (e.g. diborates) in the Li-borate glasses are thus expected to dismantle, and “loose” borate units are likely to form at higher TeO_2 contents. The term “loose” is used to describe borate tetrahedral and triangular units that are part of the glass network but do not participate in large superstructural units [37]. The presence of such borate units in the tellurite-rich glasses could possibly explain the new absorption bands peaking at about 940 and 1330 cm^{-1} for borate tetrahedral and triangular units, respectively.

The NMR results by Oliveira et al. indicate proportional sharing of lithium oxide between the borate and tellurite sub-networks, with a deviation at $x = 0.6$ and 0.8 in favor of the borate network [15]. For a glass structure based only on the proportional sharing of Li_2O with no interactions between the two sub-networks, one could assume that the spectra of the ternary glasses ($0 < x < 1$) may be expressed as appropriate linear combinations of the spectra of the end-member binary glasses, normalized by their respective molar volumes to account for differences in the number density of the borate and tellurite species [38,39]. In this respect, Fig. 4 compares measured and calculated IR spectra of ternary glasses at maximum mixing ($x = 0.5$).

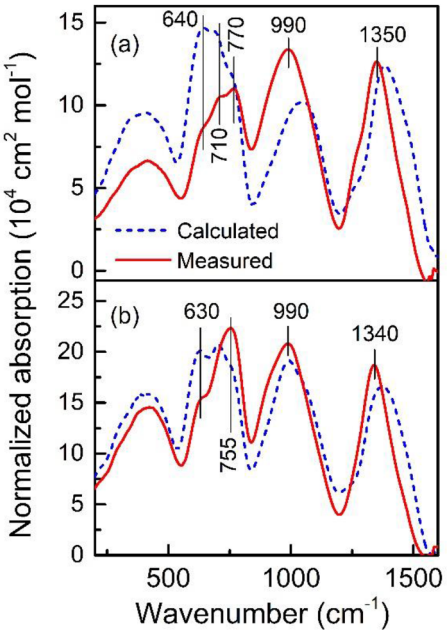

Fig. 4. Comparison of calculated spectra (weighted from the respective binary end-members) and measured IR spectra of glasses $(Li_2O)_y$-$[(2TeO_2)_{0.5}$-$(B_2O_3)_{0.5}]_{1-y}$ for $y = 0.33$ (a) and $y = 0.40$ (b). For details see text.

Clearly, there is no matching between measured and calculated infrared spectra, reflecting a mutual influence between the two sub-networks. In particular, the tellurite response in the measured spectra appears to have enhanced relative population of TeO_{3+1} and TeO_3 units with terminal oxygen atoms (bands at ca. 710 and 755–770 cm^{-1} relative to the 630–640 cm^{-1} band), implying an over-modification of the tellurite subnetwork. In addition, the change in relative intensity of the bands at 990 and 1340–1350 cm^{-1} in the measured spectra shows that the borate sub-network has an increased relative population of tetrahedral over triangular units in comparison to the calculated spectra. This result is in agreement with an increased fraction of borate tetrahedral units, N_4, found by NMR spectroscopy on the same glasses [15]. Therefore, according to both NMR and IR spectroscopies the borate tetrahedral units form in excess to those expected from a simple proportional sharing of Li_2O. The IR spectra can be employed to quantify the effect of tellurium oxide on the borate speciation by computing the integrated intensities of the absorption envelops attributed to borate tetrahedral (800–1200 cm^{-1}) and triangular (1200–1600 cm^{-1}) units, denoted as A_4 and A_3, respectively. Fig. 5 shows an example of band integration for the absorption bands corresponding to the asymmetric stretching vibration of borate tetrahedral (A_4) and borate triangular (A_3) units.

The relative integrated absorption $A_r = A_4/A_3$ is displayed as a function of tellurite content in Fig. 6. Both glass series are characterized by increasing A_r values upon TeO_2 addition, i.e. there is a progressive increase in the relative population of borate tetrahedral over triangular units at higher tellurite contents, with a steeper increase being observed for the $y = 0.33$ glass series. The knowledge of the A_r values provides the opportunity to obtain the relative absorption coefficient of boron tetrahedra over boron triangles, $\alpha_r = \alpha_4/\alpha_3$, using the following equation [25]:

$$N_4 = \frac{A_r}{a_r + A_r}, \quad (1)$$

For N_4 values we employed those by Oliveira et al. [15], adjusted to those reported by Feller at al. [40] for the two end-member Li-borate glasses ($x = 0$).

Fig. 7 provides the tellurite dependent variation of the relative absorption coefficient of borate tetrahedral over triangular units, $\alpha_r = \alpha_4/\alpha_3$, with errors in α_r resulting from the propagation of errors involved in the determination of A_r ($\delta(A_r)/A_r \sim 0.015$, this work) and N_4 ($\delta(N_4)/N_4 \sim 0.08$, ref. [15]). It is found that α_r increases as a function of tellurite content for the $y = 0.33$ glasses, giving the average value $<\alpha_r> = 1.4 \pm 0.1$. For the $y = 0.4$ series, α_r shows a minor decrease with TeO_2 content and gives the average value $<\alpha_r> = 1.7 \pm 0.1$. These results show clearly that borate tetrahedral units absorb stronger in the infrared than the borate triangles, giving the average value $<\alpha_r> = 1.6 \pm 0.1$ for the two glass series studied here. This value for the relative absorption coefficient is in good agreement with the earlier result $\alpha_r = 1.5$ obtained for Li-metaborate glass, $0.5Li_2O$-$0.5B_2O_3$ [24].

In summarizing the key aspects of this section, the evolution of the IR spectra is in full agreement with the Raman spectra and demonstrates the change in the coordination number of Te from 4 to 3 upon increasing the boron oxide content. The IR spectra shed light also on the effect of tellurium oxide on the boron speciation, demonstrating the dismantling of the rigid borate structure and the parallel conversion of borate triangular into tetrahedral units upon addition of TeO_2 to the

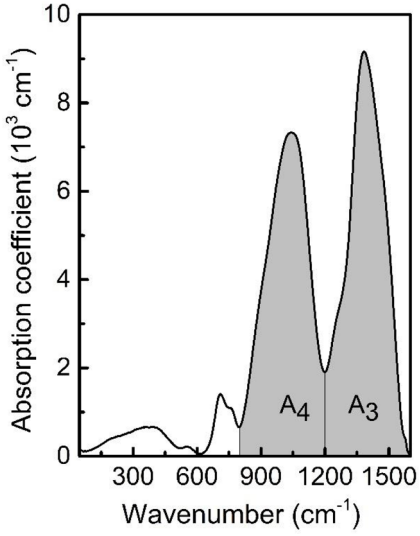

Fig. 5. Example of spectral integration for the IR absorption bands of borate tetrahedral (800–1200 cm^{-1}) and triangular (1200–1600 cm^{-1}) units of the binary $0.33Li_2O$-$0.67B_2O_3$ glass.

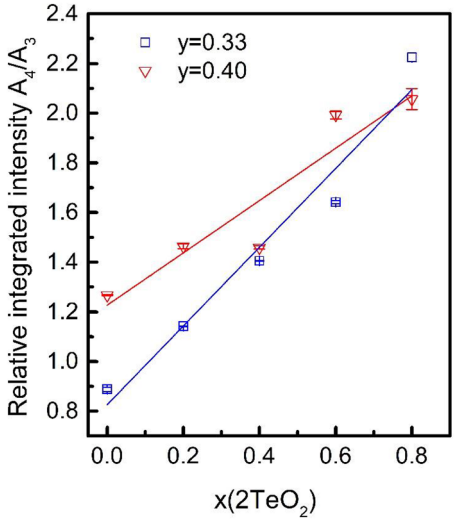

Fig. 6. Relative integrated intensity A_4 /A_3 values as a function of tellurite content for glasses $(Li_2O)_y$-$[(2TeO_2)_x$-$(B_2O_3)_{1-x}]_{1-y}$ for $y = 0.33$ and 0.40. Most error bars are of the size of data symbols or less. Lines are drawn as guides to the eye.

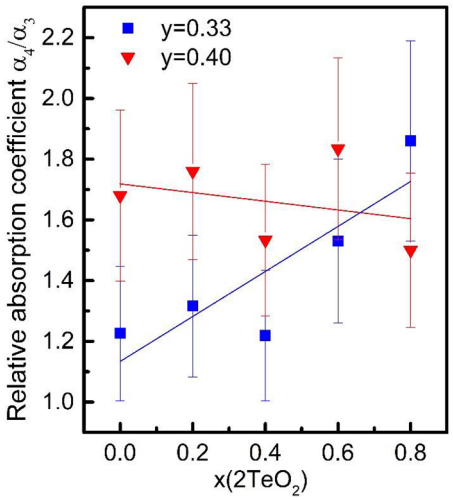

Fig. 7. Relative absorption coefficient of borate tetrahedral over triangular units, $\alpha_r = \alpha_4/\alpha_3$, as a function of tellurite content in glasses $(Li_2O)_y$-$[(2TeO_2)_x$-$(B_2O_3)_{1-x}]_{1-y}$ for $y = 0.33$ and 0.40, after calibration with B-NMR data. For details, see text. Lines are drawn as guides to the eye.

borate network. In the following we will discuss possible mechanisms for the mutual influence of the two sub-networks.

4.3. Tellurite-borate interactions in Li-boro-tellurite glasses

Assuming a proportional sharing of Li_2O between tellurite and borate sub-networks, the increase of the fraction of four-coordinated boron atoms N_4 in the ternary glasses can be considered in the context of following chemical equilibrium in the melt between the isomeric meta-borate species:

$$BO_{4/2}^- \rightleftharpoons BO_{2/2}O^- \quad (2)$$

According to the calculations of Araujo [41], this equilibrium shifts to the left upon decreasing temperature and leads to an increased fraction of the $[BO_{4/2}]^-$ species. The equilibrium constant of this isomerization reaction is principally related to the fictive temperature, but in the absence of such information the glass transition temperature (T_g) can be considered as well [42]. For the glasses investigated in this work, the T_g values decrease with increasing TeO_2 content [15], suggesting the prospective transformation of metaborate triangles, $BO_{2/2}O^-$, to metaborate tetrahedral units, $[BO_{4/2}]^-$.

In the absence of pyro- and ortho-borate units in Li-borate glasses of this study, the fractions N_2, N_3 and N_4 corresponding to the $[BO_{2/2}O]^-$, $BO_{3/2}$ and $[BO_{4/2}]^-$ units, respectively, satisfy the following equations [40,42] based on mass and charge balance:

$$N_2 + N_3 + N_4 = 1 \quad (3)$$

$$N_2 + N_4 = 1/2 \quad (4a)$$

$$N_2 + N_4 = 2/3 \quad (4b)$$

Eqs. (4a) and 4b express the total negative charge per boron centre for $y = 0.33$ and $y = 0.40$, respectively, and suggest that the maximum attainable values of N_4 are 0.50 and 0.67, respectively, in case of complete isomerization of $[BO_{2/2}O]^-$ to $[BO_{4/2}]^-$ (Eq. (2)). However, the reported N_4 values for the tellurite-rich glass ($x = 0.8$) are 0.61 for $y = 0.33$ and 0.70 for $y = 0.40$ [15], i.e. higher than the maximum attainable values for borate modification based on the entire Li_2O content available. It is thus deduced that borate modification based only on the lithium oxide modifier and the isomerization of metaborate triangles to tetrahedral units cannot adequately account for the high N_4 values. This inevitably points towards consideration of an alternative mechanism that may involve direct interaction of the two sub-networks, in accordance to the suggestions by Oliveira et al. [15].

Indeed, a TeO_2–induced formation of borate tetrahedra can be rationalized in terms of the Lewis acid-base properties of the B_2O_3 and TeO_2 oxides as discussed recently [34]. Since the optical basicity (Λ) values of TeO_2 and B_2O_3 are 0.99 and 0.43 [30], respectively, tellurium oxide can act as a Lewis base (electron donor) and boron oxide as a Lewis acid (electron acceptor). This suggests that the relatively basic TeO_2 can function as a second modifier (besides Li_2O) on the more acidic B_2O_3. This change of role for TeO_2 from glass former to glass modifier is not surprising as it exhibits very similar optical basicity to Li_2O ($\Lambda = 1.0$). Also, this role of tellurium oxide is in line with the large difference in bond strength energies between the Te-O and B-O bonds with $E_{Te\text{-}O} = 390.8 \pm 8.4$ kJ/mol and $E_{B\text{-}O} = 806.3 \pm 5.0$ kJ/mol [43], implying a glass modifier function of TeO_2 in the presence of B_2O_3 [44]. The formation of $[BO_{4/2}]^-$ units by TeO_2 addition to B_2O_3 can be described by the following reaction:

$$TeO_2 + \tfrac{1}{2}B_2O_3 \rightarrow TeO_{3/2}^+ \ldots O(\text{-}BO)^- \quad (5)$$

According to Eq. (5), tellurium is assumed to keep its four-fold coordination through formation of an elongated Te…O bond, which is responsible for providing the required oxygen atoms for the modification of B_2O_3 [16,34,45]. This elongated bond is weaker than the other three Te-O bonds on the $TeO_{3/2}$ …O tellurite unit. The latter units can be considered as distorted $TeO_{4/2}$ units with vibrational signatures close to those of TeO_{3+1} [34]. The $O(\text{-}BO)^-$ notation in Eq. (5) indicates tetrahedral $[BO_{4/2}]^-$ and/or triangular $[BO_{2/2}O]^-$metaborate species.

On the other hand, addition of B_2O_3 leads to the progressive formation of negatively charged TeO_3 tellurite units. Due to the constant amount of lithium oxide available, an additional modification mechanism is required for the development of such TeO_3 units. We suggest that part of the $TeO_{3/2}^+ \ldots O(\text{-}BO)^-$ units can be modified by lithium oxide as described by the following reaction:

$$TeO_{3/2}^+ \ldots O(\text{-}BO)^- + Li_2O \rightarrow (TeO_{1/2}O_2)^- \ldots Li^+ + (BO_2)^- \ldots Li^+ \quad (6)$$

In Eq. (6), $(TeO_{1/2}O_2)^-$ represents a negatively charged TeO_3 unit with two terminal oxygen atoms and $(BO_2)^-$ is a borate tetrahedral $[BO_{4/2}]^-$ unit and/or trigonal $[BO_{2/2}O]^-$ unit.

Therefore, interaction among the two sub-networks appears to provide reasonable mechanisms and structural models for the understanding and interpretation of the Raman and IR spectra, although there was no detection of specific vibrational features assigned to the weak Te…O-B linkages. The decrease of the glass transition temperature and its negative deviation from linearity upon increasing the TeO_2 content (see Fig. S1 of ref. [15]), is an indication of the building up of rather weak Te…O-B linkages between the two sub-networks.

5. Conclusion

This work has focused on the investigation of ternary lithium borotellurite glasses with composition $(Li_2O)_y$-$[(2TeO_2)_x$-$[(B_2O_3)_{1-x}]_{1-y}$ ($y = 0.33$, 0.40 and $0 \le x \le 1$) by means of Raman and IR spectroscopies. The Raman spectra demonstrate the progressive transition from TeO_4 to negatively charged TeO_3 structural units with terminal oxygen atoms at increasing boron oxide content and the formation of distorted TeO_4 units with elongated Te…O bonds, such units being associated to the vibrational activity emerging at ~745 cm^{-1}. The presence of these distorted tellurite units provides new insights into the interaction of the two glass sub-networks through weak Te…O-B bonds. However, due to their high scattering cross section, the tellurite vibrational modes dominate the Raman spectra and very limited information is obtained for the structure of the borate units. On the contrary, the IR spectra exhibit distinct absorption features assigned to borate tetrahedra and borate triangles, with the former species gaining relative population as a function of TeO_2 inclusion. In addition, the borate absorption

envelopes in the IR were found to exhibit variations in shape and frequency upon increasing the tellurite content. This finding was discussed in terms of the effect of the large tellurium atoms on the borate subnetwork, leading to the disassembling of the borate superstructural groups and the creation of "loose" borate units.

We suggest that the described structural changes can be explained on the basis of weak interactions among the two sub-networks, where TeO_2 can act also as a second modifier on B_2O_3 due to their difference in optical basicity. A modification mechanism is proposed to account for the "excess" formation of tetrahedral $[BO_{4/2}]^-$ units; it involves distorted TeO_4 units with elongated Te…O bonds leading to the formation of weak Te…O-B linkages and the additional borate modification. Overall, these results highlight the need for complementary use of Raman and IR techniques to investigate and understand the structure of multicomponent glass systems.

CRediT authorship contribution statement

K.I. Chatzipanagis: Investigation, Formal analysis, Writing - original draft, Writing - review & editing. **N.S. Tagiara:** Investigation, Writing - review & editing. **D. Möncke:** Conceptualization, Investigation, Writing - review & editing. **S. Kundu:** Investigation. **A.C.M. Rodrigues:** Conceptualization, Investigation, Writing - review & editing, Funding acquisition. **E.I. Kamitsos:** Conceptualization, Supervision, Funding acquisition, Formal analysis, Writing - review & editing, Project administration.

Declaration of Competing Interest

The authors declare no competing interests.

Acknowledgements

This work was supported by the project "National Infrastructure in Nanotechnology, Advanced Materials and Micro - / Nanoelectronics" (MIS 5002772) which is implemented under the Action "Reinforcement of the Research and Innovation Infrastructure", funded by the Operational Program "Competitiveness, Entrepreneurship and Innovation" (NSRF 2014–2020) and co-financed by Greece and the European Union (European Regional Development Fund). We also acknowledge the financial support of FAPESP grant (São Paulo Research Foundation, number 2017/02953–w6 and 2013/07793w, CeRTEV-CEPID program), and CAPES project number 88881.068006/2014–01. We are grateful also to Dr. E. Chrysina and Dr. M-D. Charavgi for XRD measurements at the Institute of Chemical Biology of NHRF, in the framework of the project "INSPIRED-The National Research Infrastructures on Integrated Structural Biology, Drug Screening Efforts and Drug target functional characterization" (MIS 5002550, NSRF 2014–2020).

References

[1] H. Bürger, W. Vogel, V. Kozhukharov, IR transmission and properties of glasses in the TeO_2-R_nO_m, R_nX_m, $R_n(SO_4)_m$, $R_n(PO_3)_m$ and B_2O_3] systems, Infrared Phys. 25 (1985) 395–409.
[2] M.J. Weber, Science and technology of laser glass, J. Non-Cryst. Solids 123 (1990) 208–222.
[3] E.M. Vogel, M.J. Weber, D.M. Krol, Nonlinear optical phenomena in glass, Phys. Chem. Glasses 32 (1991) 231–254.
[4] R.A.H. El-Mallawany, Tellurite Glasses Handbook: Physical Properties and Data, CRC Press, Boca Raton, FL, USA, 2002.
[5] Y. Ito, K. Miyauchi, T. Oi, Ionic conductivity of Li_2O-B_2O_3 thin films, J. Non-Cryst. Solids 57 (1983) 389–400.
[6] T. Minami, Fast ion conducting glasses, J. Non-Cryst. Solids 73 (1985) 273–284.
[7] E.I. Kamitsos, A.P. Patsis, M.A. Karakassides, G.D. Chryssikos, Infrared reflectance spectra of lithium borate glasses, J. Non-Cryst. Solids 126 (1990) 52–67.
[8] T. Minami, A. Hayashi, M. Tatsumisago, Recent progress of glass and glass-ceramics as solid electrolytes for lithium secondary batteries, Solid State Ionics 177 (2006) 2715–2720.
[9] M. Dussauze, E.I. Kamitsos, P. Johansson, A. Matic, C.P.E. Varsamis, D. Cavagnat, P. Vinatier, Y. Hamon, Lithium ion conducting boron-oxynitride amorphous thin films: synthesis and molecular structure by infrared spectroscopy and density functional theory modeling, J. Phys. Chem. C. 117 (2013) 7202–7213.
[10] B. Raguenet, G. Tricot, G. Silly, M. Ribes, A. Pradel, The mixed glass former effect in twin-roller quenched lithium borophosphate glasses, Solid State Ionics 208 (2012) 25–30.
[11] D. Larink, H. Eckert, M. Reichert, S.W. Martin, Mixed network former effect in ion-conducting alkali borophosphate glasses: structure/property correlations in the system $[M_2O]_{1/3}[(B_2O_3)_x(P_2O_5)_{1-x}]_{2/3}$ (M = Li, K, Cs), J. Phys. Chem. C. 116 (2012) 26162–26176.
[12] A.C. Wright, My borate life: an enigmatic journey, Int. J. Appl. Glas. Sci. 6 (2015) 45–63.
[13] D. Larink, M.T. Rinke, H. Eckert, Mixed network former effects in tellurite glass systems: structure/property correlations in the system $(Na_2O)_{1/3}[(2TeO_2)_x(P_2O_5)_{1-x}]_{2/3}$, J. Phys. Chem. C. 119 (2015) 17539–17551.
[14] D. Larink, H. Eckert, Mixed network former effects in tellurite glass systems: structure/property correlations in the system $(Na_2O)_{1/3}[(2TeO_2)_x(B_2O_3)_{1-x}]_{2/3}$, J. Non-Cryst. Solids 426 (2015) 150–158.
[15] M. de Oliveira, J.S. Oliveira, S. Kundu, N.M.P. Machado, A.C.M. Rodrigues, H. Eckert, Network former mixing effects in ion-conducting lithium borotellurite glasses: structure/property correlations in the system $(Li_2O)_y[2(TeO_2)_x(B_2O_3)_{1-x}]_{1-y}$, J. Non-Cryst. Solids 482 (2018) 14–22.
[16] Q.J. Rong, A. Osaka, T. Nanba, J. Takada, Y. Miura, Infrared and Raman spectra of binary tellurite glasses containing boron and indium oxides, J. Mater. Sci. 27 (1992) 3793–3798.
[17] T. Sekiya, N. Mochida, A. Ohtsuka, M. Tonokawa, Raman spectra of $MO_{1/2}$-TeO_2 (M = Li, Na, K, Rb, Cs an Tl) glasses, J. Non-Cryst. Solids 144 (1992) 128–144.
[18] M. Tatsumisago, S.K. Lee, T. Minami, Y. Kowada, Raman spectra of TeO_2-based glasses and glassy liquids: local structure change with temperature in relation to fragility of liquid, J. Non-Cryst. Solids 177 (1994) 154–163.
[19] T. Sekiya, N. Mochida, A. Soejima, Raman spectra of binary tellurite glasses containing tri- or tetra-valent cations, J. Non-Cryst. Solids 191 (1995) 115–123.
[20] N.S. Tagiara, D. Palles, E.D. Simandiras, V. Psycharis, A. Kyritsis, E.I. Kamitsos, Synthesis, thermal and structural properties of pure TeO_2 glass and zinc-tellurite glasses, J. Non-Cryst. Solids 457 (2017) 116–125.
[21] W.L. Konijnendijk, J.M. Stevels, The structure of borate glasses studied by Raman scattering, J. Non-Cryst. Solids 18 (1975) 307–331.
[22] E.I. Kamitsos, M.A. Karakassides, G.D. Chryssikos, A vibrational study of lithium borate glasses with high Li_2O content, Phys. Chem. Glasses 28 (1987) 203–209.
[23] E.I. Kamitsos, M.A. Karakassides, G.D. Chryssikos, Vibrational spectra of magnesium-sodium-borate glasses. 2. Raman and mid-infrared investigation of the network structure, J. Phys. Chem. 91 (1987) 1073–1079.
[24] G.D. Chryssikos, J.A. Kapoutsis, E.I. Kamitsos, A.J. Patsis, A.J. Pappin, Lithium-sodium metaborate glasses: structural aspects and vitrification chemistry, J. Non-Cryst. Solids 167 (1994) 92–105.
[25] Y.D. Yiannopoulos, G.D. Chryssikos, E.I. Kamitsos, Structure and properties of alkaline earth borate glasses, Phys. Chem. Glasses 42 (2001) 164–172.
[26] D. Möncke, E.I. Kamitsos, D. Palles, R. Limbach, A. Winterstein-Beckmann, T. Honma, Z. Yao, T. Rouxel, L. Wondraczek, Transition and post-transition metal ions in borate glasses: borate ligand speciation, cluster formation, and their effect on glass transition and mechanical properties, J. Chem. Phys. 145 (2016) 124501/1-16.
[27] V.V. Sinitsyn, B.S. Red'kin, V.I. Orlov, O.F. Shakhlevich, N.N. Kolesnikov, X-ray diffraction, calorimetric, and spectroscopic studies of lithium borate glass activated with various oxide admixtures based on europium, Glass Phys. Chem. 42 (2016) 453–457.
[28] N. Kaur, A. Khanna, Structural characterization of borotellurite and alumino-borotellurite glasses, J. Non-Cryst. Solids 404 (2014) 116–123.
[29] E.I. Kamitsos, Infrared spectroscopy of glasses, in: M. Affatigato (Ed.), Mod. Glas. Charact. John Wiley & Sons, New York, 2015, pp. 32–73 (Chapter 2).
[30] V. Dimitrov, S. Sakka, Electronic oxide polarizability and optical basicity of simple oxides. I, J. Appl. Phys. 79 (1996) 1736–1740.
[31] F.L. Galeener, G. Lucovsky, J.C. Mikkelsen Jr, Vibrational spectra and the structure of pure vitreous B_2O_3, Phys. Rev. B. 22 (1980) 3983–3990.
[32] C.F. Windisch, W.M. Risen, Vibrational spectra of oxygen- and boron-isotopically substituted B_2O_3 glasses, J. Non-Cryst. Solids 48 (1982) 307–323.
[33] T. Sekiya, N. Mochida, A. Ohtsuka, A. Soejima, Raman spectra of $BO_{3/2}$-TeO_2 glasses, J. Non-Cryst. Solids 151 (1992) 222–228.
[34] N.S. Tagiara, E. Moayedi, A. Kyritsis, L. Wondraczek, E.I. Kamitsos, Short-range structure, thermal and elastic properties of binary and ternary tellurite glasses, J. Phys. Chem. B. 123 (2019) 7905–7918.
[35] G.D. Chryssikos, L. Liu, C.P. Varsamis, E.I. Kamitsos, Dielectric and structural investigation of alkali triborate glasses, J. Non. Cryst. Solids 235–237 (1998) 761–765.
[36] Y.B. Saddeek, H.A. Afifi, N.S. Abd El-Aal, Interpretation of mechanical properties and structure of TeO_2-Li_2O-B_2O_3 glasses, Phys. B Condens. Matter. 398 (2007) 1–7.
[37] Y.H. Yun, P.J. Bray, B^{11} nuclear magnetic resonance studies of Li_2O-B_2O_3 glasses of high Li_2O content, J. Non-Cryst. Solids 44 (1981) 227–237.
[38] E.I. Kamitsos, A.P. Patsis, G.D. Chryssikos, Interactions between cations and the network in mixed alkali borate glasses, Phys. Chem. Glasses 32 (1991) 219–221.
[39] E.I. Kamitsos, A.P. Patsis, G.D. Chryssikos, Infrared reflectance investigation of alkali diborate glasses, J. Non-Cryst. Solids 152 (1993) 246–257.
[40] S.A. Feller, W.J. Dell, P.J. Bray, ^{10}B NMR studies of lithium borate glasses, J. Non-Cryst. Solids 51 (1982) 21–30.
[41] R.J. Araujo, Statistical mechanics of chemical disorder: application to alkali borate

glasses, J. Non-Cryst. Solids 58 (1983) 201–208.
[42] C.P. Varsamis, E.I. Kamitsos, G.D. Chryssikos, Structure of fast-ion-conducting AgI-doped borate glasses in bulk and thin film forms, Phys. Rev. B 60 (1999) 3885–3898.
[43] CRC, *Handbook of Chemistry and Physics*, 60 Edition, (1980) Boca Raton, Florida, USA.
[44] A. Mirgorodsky, M. Colas, M. Smirnov, T. Marle-Mejean, R. El-Mallawany, P. Thomas, Structural peculiarities and Raman spectra of TeO_2/WO_3-based glasses: a fresh look at the problem, J. Solid State Chem. 190 (2012) 45–51.
[45] H. Bürger, W. Vogel, V. Kozhukharov, M. Marinov, Phase equilibrium, glass-forming, properties and structure of glasses in the TeO_2-B_2O_3 system, J. Mater. Sci. 19 (1984) 403–412.